ELSEVIER

Catalysis Today 69 (2001) 75–85

CATALYSIS TODAY

www.elsevier.com/locate/cattod

Determination of catalytic packing characteristics for reactive distillation

Andrzej Kołodziej [a,*], Mieczysław Jaroszyński [a], Achim Hoffmann [b], Andrzej Górak [b]

[a] *Institute of Chemical Engineering, Polish Academy of Sciences, ul. Baltycka 5, 44-100 Gliwice, Poland*
[b] *Department of Chemical, Mechanical and Energy Engineering, Essen University, Essen, Germany*

Abstract

Catalytic distillation still expands its field of applications. New structured catalytic column internals have been developed in recent years and new studies have been reported. A modern structured catalytic packing MULTIPAK® is a subject of the investigations presented in this paper.

Important parameters of MULTIPAK® have been examined experimentally in a 250 mm ID laboratory column: pressure drop for dry, prewetted and irrigated packings, flooding line and mass transfer coefficients for the gas and liquid phases.

The correlations obtained have been incorporated into a software tool for the simulation of catalytic distillation processes and simulations have been performed assuming methyl acetate synthesis as a model process. The calculations have been verified using the experiments performed for the same synthesis in a 50 mm ID catalytic distillation column operating continuously and thus reflecting industrial applications. It is concluded that the model represents the real process with satisfactory accuracy, although some deviations can be observed, especially within the reactive zone.

Keywords: MULTIPAK®; Catalytic distillation; Reactive distillation

1. Introduction

In recent years, reactive distillation has been gaining increasing attention in both the industrial practice and scientific research. Advantages of this technology are obvious: environmental protection, reduction of investment costs, lower energy consumption. Nowadays, the heterogeneously catalysed reactive distillation, the so-called catalytic distillation, seems to be the most promising one. In recent years, some new types of column packing have been developed specifically for the catalytic distillation. Extensive experimental work has been performed to investigate the behaviour of catalytic column internals like KATAPAK®-S [1]. The reactive distillation is, however, a very complex process and its design is much more complicated than that for the individual processes, such as chemical reaction or distillation; it is a mathematical modelling rather than conventional design.

The aim of the project is to develop a method which would allow the design of catalytic distillation columns. In order to reach this objective, the following tasks have been specified:

- determination of the pressure drop, flooding point and mass transfer coefficients;
- development of correlation equations;
- implementation of the correlation equations into the simulation software tool for the design of catalytic distillation processes;

* Corresponding author. Tel.: +48-32-2310-811; fax: +48-32-2310-318.
E-mail address: ask@iich.gliwice.pl (A. Kołodziej).

0920-5861/01/$ – see front matter
PII: S0920-5861(01)00357-1

Nomenclature

a	specific surface area (m^2/m^3)
A	surface area of mass transfer (m^2)
d_e	hydraulic packing diameter (m)
D_c	column diameter (m)
$F = w_{0g}\rho_g{}^{0.5}$	F-factor ($Pa^{0.5}$)
g	acceleration of gravity (m/s^2)
g_0	mass superficial velocity ($kg/(m^2\,s)$)
G	flow rate (kmol/s)
H	column height (m)
H_P	Henry's law constant (Pa)
k_A	overall mass transfer coefficient ($kmol/(m^2\,s)$)
K	wall factor (dimensionless)
M	molecular mass (kg/kmol)
n	modified slope of the equilibrium curve (dimensionless)
N	molar diffusive flow (kmol/s)
p	partial pressure (Pa)
ΔP	pressure drop (Pa)
r	reaction rate (kmol/(kg s))
$Re = g_0 d_e/\varepsilon\eta$	Reynolds number
$Re_{gK} = g_0 d_e K/\varepsilon\eta_g$	gas-phase Reynolds number used in hydraulic experiments
$Sc = \eta/\delta M$	Schmidt number
$Sh_g = \beta_A d_e/\delta_A$	gas-phase Sherwood number
$Sh_L = \beta_A \vartheta_z/\delta_A$	liquid-phase Sherwood number
w_0	superficial velocity (m/s)
x, y	mole fraction (liquid and gas phases, respectively) (dimensionless)
X, Y	molar ratio (liquid and gas phases, respectively) (dimensionless)
Δz	height of the stage of the column (m)

Greek letters

β_A	individual mass transfer coefficient ($kmol/(m^2 s)$)
δ_A	dynamic diffusivity (kmol/(m s))
ε	void fraction (m^3/m^3)
η	dynamic viscosity (Pa s)
$\vartheta_z = (\eta^2/\rho^2 g)^{1/3}$	equivalent linear dimension (m)
$\Delta\pi_A$	driving force (dimensionless)
ρ	density (kg/m^3)
Ψ	friction factor (dimensionless)

Subscripts

A	diffusing species
g	gas phase
i	ith component
in	interface
inert	inert component
L	liquid phase
m	mean
t	total (sum of all the components)
w	water

Superscripts

j	jth stage of column
$*$	the gas-phase concentration in equilibrium with the liquid concentration

- validation of the software based on the appropriate experimental results.

2. Reactive packing investigated

A catalytic packing investigated was MULTIPAK® manufactured by Julius Montz GmbH, Germany (Fig. 1). MULTIPAK® has a sandwich structure of corrugated wire gauze sheets and vertical catalyst pockets filled with cation-exchange resin of the type Lewatit K2621. The specific data for the packing were determined experimentally during this study: specific surface area $a = 320\,m^2/m^3$ and void fraction $\varepsilon = 0.65\,m^3/m^3$.

3. Experimental procedure

The studies have been performed in a column 250 mm in diameter and packing heights up to 1 m, for the liquid superficial mass velocities g_{0L} from 0.26 to 25.8 $kg/(m^2\,s)$ and the gas superficial velocities w_{0g} from 0.3 to 3 m/s. The air–water system was

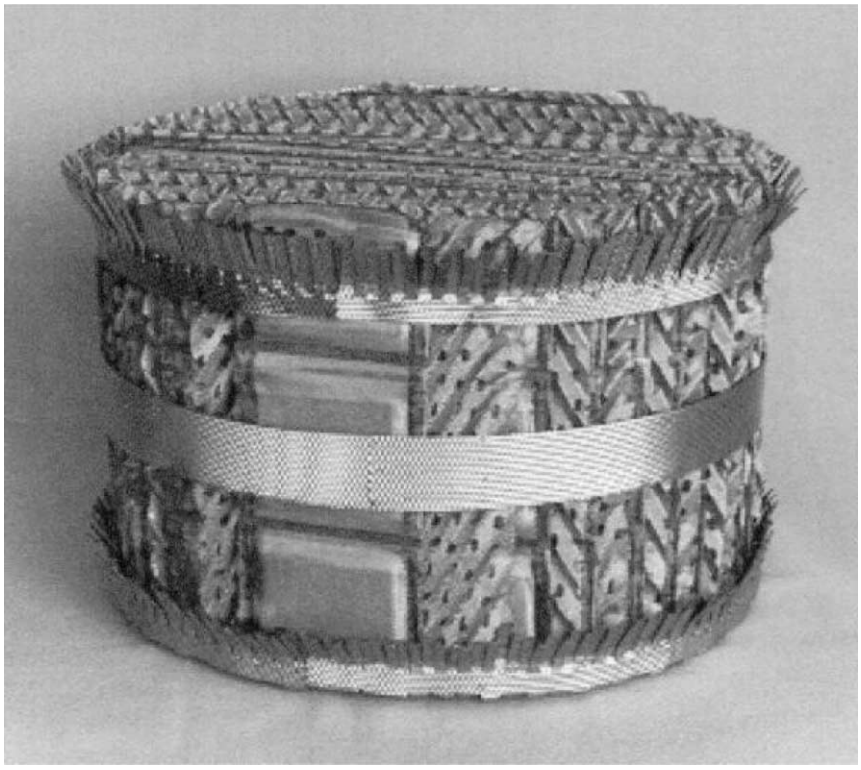

Fig. 1. Structured catalytic packing MULTIPAK®.

used. The experimental setup is presented in Fig. 2. The liquid flowing from tanks through a pump and flowmeters was supplied into the column via a distributor. After passing the packing layer, it was collected in the bottom of the column and removed. The air stream came into the bottom of the column from a blower through an orifice flowmeter. Due to very low liquid flow rates in some experiments, it was necessary to saturate the gas phase with the water vapour using a saturator. After passing the packing, the gas was removed from the column top.

During the liquid-phase mass transfer experiments, a carbon dioxide circuit was used as shown in Fig. 2. Liquid in the tanks was saturated with CO_2 from gas cylinders via flowmeters and bubblers; the desorption of CO_2 from water to the air stream occurred in the column. The concentrations of carbon dioxide in the liquid below and above the packing layer were determined by titration.

In the gas-phase mass transfer experiments, an ammonia circuit supplied NH_3 from cylinders through a calibrated flowmeter into the air stream entering the column. Absorption of ammonia took place inside the packing. The inlet concentration in the gas phase was determined based on the flow rates of the air and ammonia streams, while the outlet concentration by titrating samples of the absorbed gas.

Due to a very wide range of liquid flow rates during the experiments, three different capillary liquid distributors were used with various capillary diameters; all had 1366 holes per square metre.

4. Experimental results: hydraulics

In contrast to the common approach to the pressure drop in packed columns, it was necessary to distinguish three flow regimes: *dry packing* — single-phase gas flow through the dry packing; *prewetted packing* — single-phase gas flow through the prewetted packing; *wetted* (*irrigated*) *packing* — two-phase counter-current gas and liquid flow (the usual

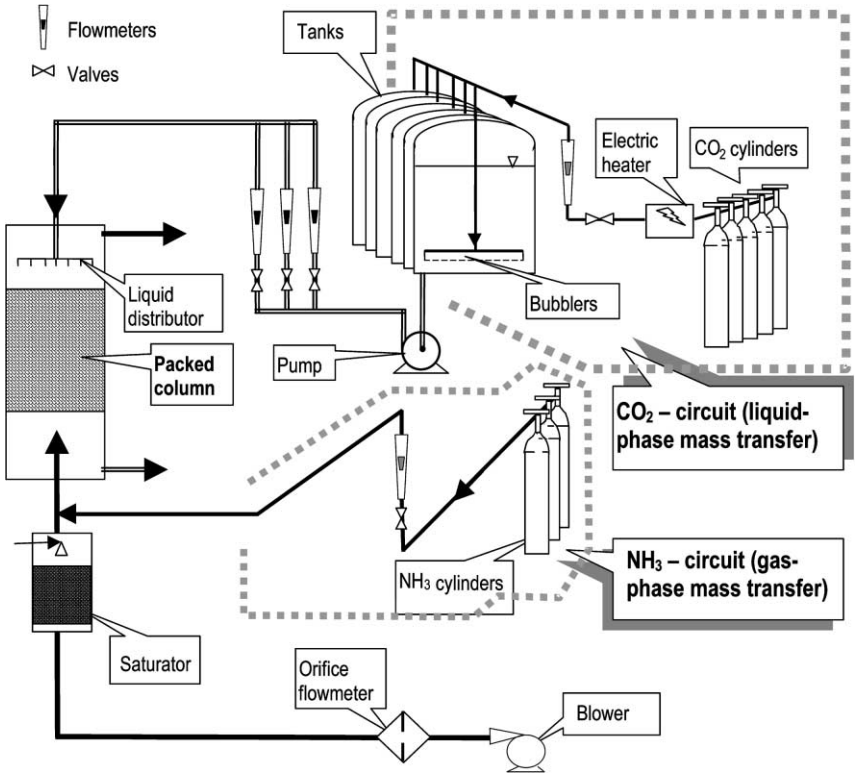

Fig. 2. Experimental setup for hydraulic and mass transfer studies.

working regime of a packed column). The distinction was necessary due to considerable differences between the pressure drops for the dry and prewetted packings — the former were much higher, especially for the high gas velocities.

The pressure drop for the dry (prewetted) packing can be calculated from the Darcy–Weisbach equation

$$\frac{\Delta P}{H} = \Psi \frac{\rho_g w_{0g}^2}{2\varepsilon^2 d_e K} \tag{1}$$

The hydraulic packing diameter d_e and the wall factor K can be defined as [2]:

$$d_e = \frac{4\varepsilon}{a}, \qquad K = \frac{1}{1 + 4/(aD_c)} \tag{2}$$

and, consequently

$$\frac{\Delta P}{H} = \Psi \frac{a\rho_g w_{0g}^2}{8\varepsilon^3 K} \tag{3}$$

The experimental data obtained for the two one-phase flows are presented in Fig. 3; they have been correlated using the Ψ parameter as follows:

$$\Psi_{dry} = 12.88\, Re_{gK}^{-0.386} \quad \text{for} \quad Re_{gK} \le 515,$$
$$\Psi_{dry} = 1.159 \quad \text{for} \quad Re_{gK} > 515 \tag{4}$$

$$\Psi_{prewetted} = 16.13\, Re_{gK}^{-0.436} \quad \text{for} \quad Re_{gK} \le 710,$$
$$\Psi_{prewetted} = 3.210\, Re_{gK}^{-0.189} \quad \text{for} \quad Re_{gK} > 710 \tag{5}$$

The scatter of the experimental points around the correlation line does not exceed 5%.

The pressure-drop data for the irrigated packing are presented in Fig. 4 in terms of $\Delta P/H$ vs. gas F-factor and liquid load (the results for the prewetted regime are also included in this figure).

The flooding line, which is a very important design parameter for the packed columns, was determined

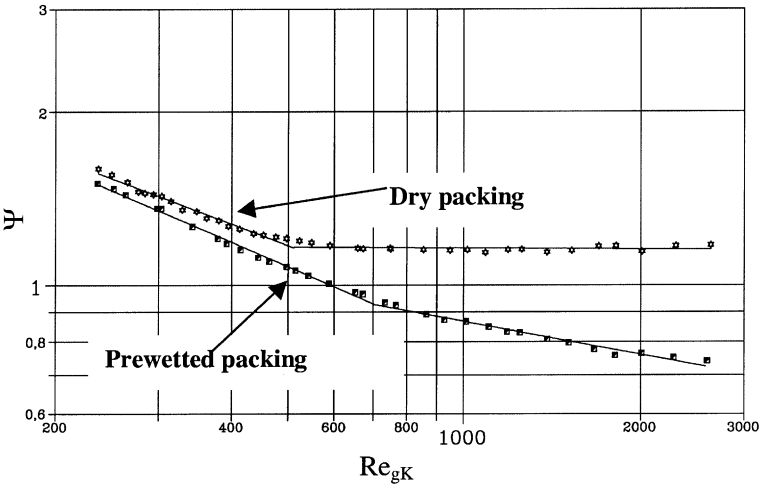

Fig. 3. Friction factor vs. gas Reynolds number for dry and prewetted flow regimes.

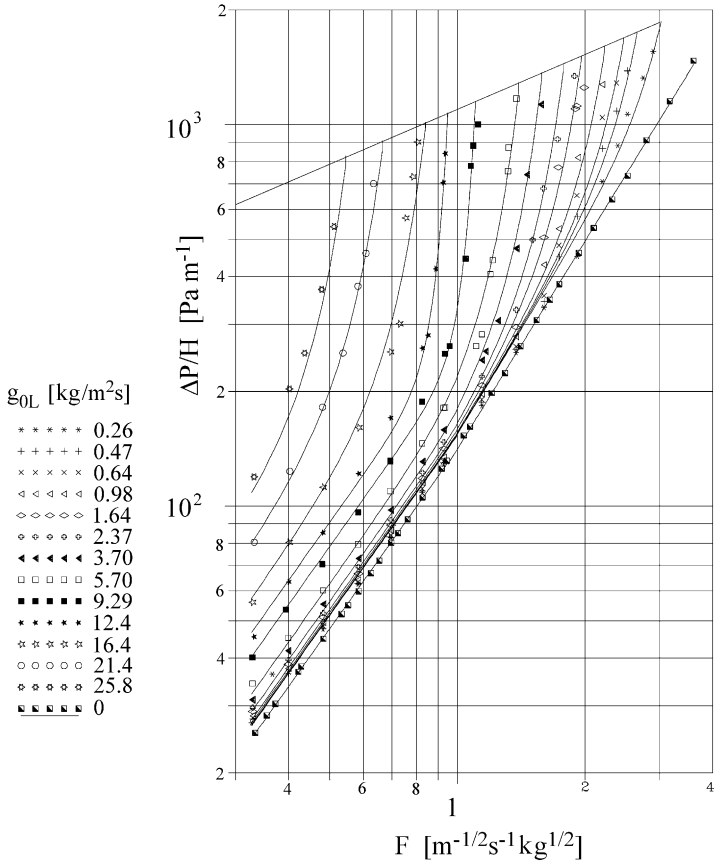

Fig. 4. Pressure drop vs. gas *F*-factor for various liquid loads (irrigated packing).

based on visual observations of the process and correlated as

$$\frac{\Delta P_{\text{prewetted}}\eta_{\text{w}}^{0.2}}{\rho_{\text{L}}gH} = 0.210\exp\left[-3.36\left(\frac{g_{0\text{L}}}{g_{0\text{g}}}\right)^{1/4}\left(\frac{\rho_{\text{g}}}{\rho_{\text{L}}}\right)^{1/8}\right] \quad (6)$$

5. Experimental results: mass transfer — liquid phase

The driving forces in the two cross-sections were calculated according to Hobler [3] as:

$$\beta_{\text{AL}} = \frac{G_{\text{inert}}(X_{\text{A2}} - X_{\text{A1}})}{A\Delta\pi_{\text{Am}}} \quad (7)$$

$$\Delta\pi_{\text{A}} = \frac{X_{\text{A}} - X_{\text{A in}}}{(1 + X_{\text{A}})_{\text{m}}} \approx X_{\text{A}} - X_{\text{A in}} \quad (X_{\text{A}} \ll 1) \quad (8)$$

Using Henry's law to determine the concentrations at the gas–liquid interface

$$X_{\text{A in}} \approx x_{\text{A in}} = \frac{p_{\text{A}}}{H_{\text{P}}} \quad (9)$$

Due to a very high value of the Henry's law constant for the carbon dioxide–water system, the mass transfer resistance in the gas phase is negligible [4]. The mass transfer surface area A was assumed to be identical with the geometrical surface area of the packing.

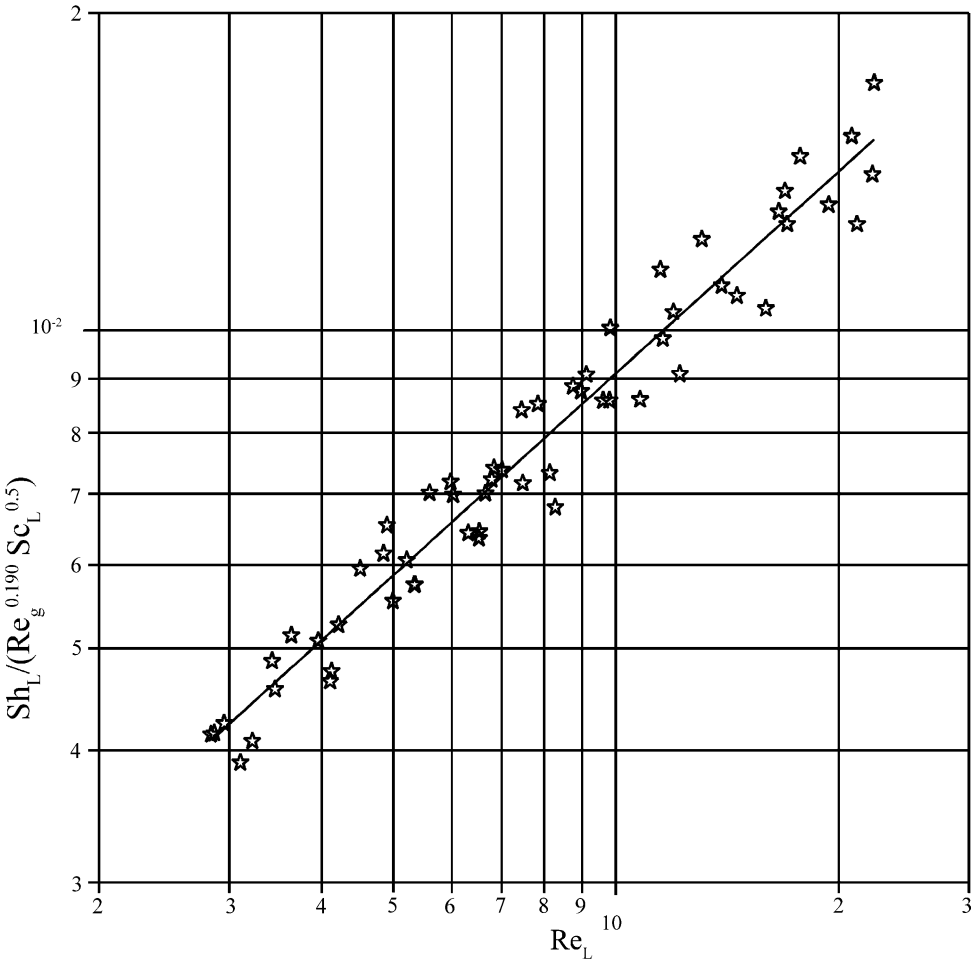

Fig. 5. Liquid-phase mass transfer coefficients: Sherwood number vs. liquid Reynolds number — lower range.

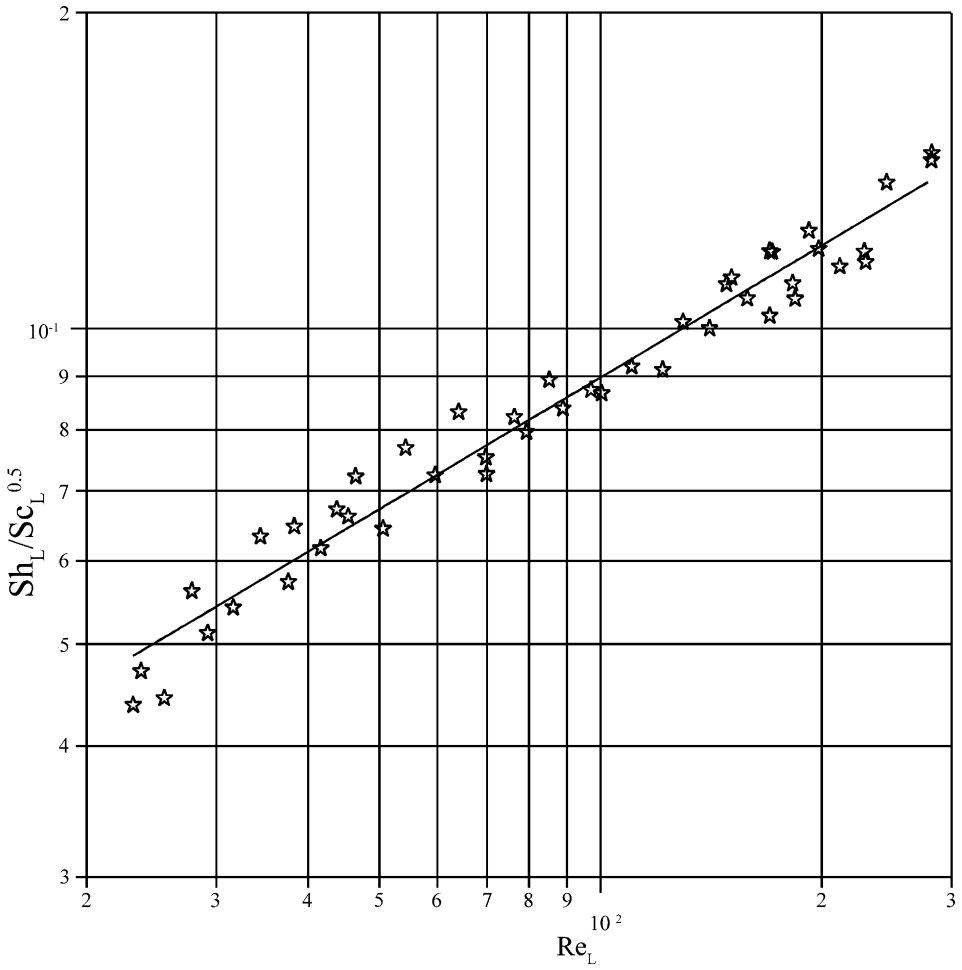

Fig. 6. Liquid-phase mass transfer coefficients: Sherwood number vs. liquid Reynolds number — upper range.

The results obtained are presented in Figs. 5 and 6; they are correlated as

$$Sh_L = 0.0021\, Re_L^{0.636}\, Re_g^{0.190} Sc_L^{0.5} \quad \text{for} \quad 2.83 \le Re_L \le 23 \tag{10}$$

$$Sh_L = 0.0131\, Re_L^{0.418} Sc_L^{0.5} \quad \text{for} \quad 23 < Re_L \le 282 \tag{11}$$

The scatter of the experimental points around the correlation line does not exceed 15%. The exponent at the Schmidt number was taken from the literature by analogy to other studies due to only small changes of this number in the present study.

6. Experimental results: mass transfer — gas phase

The overall mass transfer coefficient can be derived from the balance of the diffusing species

$$k_A = \frac{G_{inert}\,(Y_{A2} - Y_{A1})}{A(\Delta\pi_A)_m} \quad \text{where} \quad \Delta\pi_A = \ln\frac{1+Y_A}{1+Y_A^*} \tag{12}$$

The gas-phase mass transfer coefficient can then be expressed as

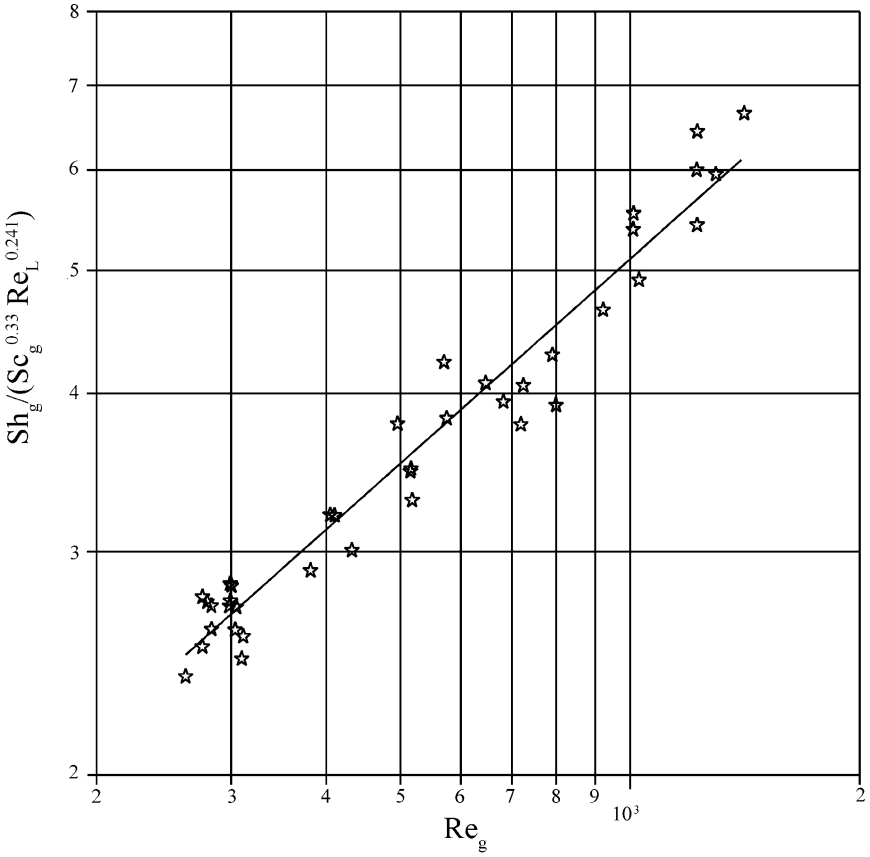

Fig. 7. Gas-phase mass transfer coefficients: Sherwood number vs. gas Reynolds number — lower range.

$$\beta_{Ag} = \frac{1}{(1/k_A) - (n/\beta_{AL})} \tag{13}$$

For the absorption of ammonia in water, the liquid-phase mass transfer resistance is usually an order of magnitude lower in comparison with that in the gas phase; nevertheless, the liquid-phase mass transfer coefficients have been calculated from correlations (10) and (11) and substituted into Eq. (13).

The results obtained are presented in Figs. 7 and 8 and have been correlated as

$$Sh_g = 0.126\,Re_g^{0.536}\,Re_L^{0.241}\,Sc_g^{0.33} \quad \text{for} \quad 2.92 \le Re_L \le 23 \tag{14}$$

$$Sh_g = 0.156\,Re_g^{0.618}\,Sc_g^{0.33} \quad \text{for} \quad 23 < Re_L \le 292 \tag{15}$$

The scatter of the experimental points around the correlation line does not exceed 15%. The exponent at the Schmidt number was taken from the literature by analogy to other studies due to only small changes of this number in the present study.

In the present study, mass transfer coefficients were determined based on the geometrical surface area of the packing. Therefore, Eqs. (10), (11), (14) and (15) represent the effect of the gas and liquid Reynolds numbers on both the individual mass transfer coefficients and the effective contact area between the gas and the liquid. Such an approach required the measurements to be conducted over the whole admissible range of loads for the two phases. Such an approach makes it possible to avoid the use of correlations for the surface effectiveness factor (wetting factor) which

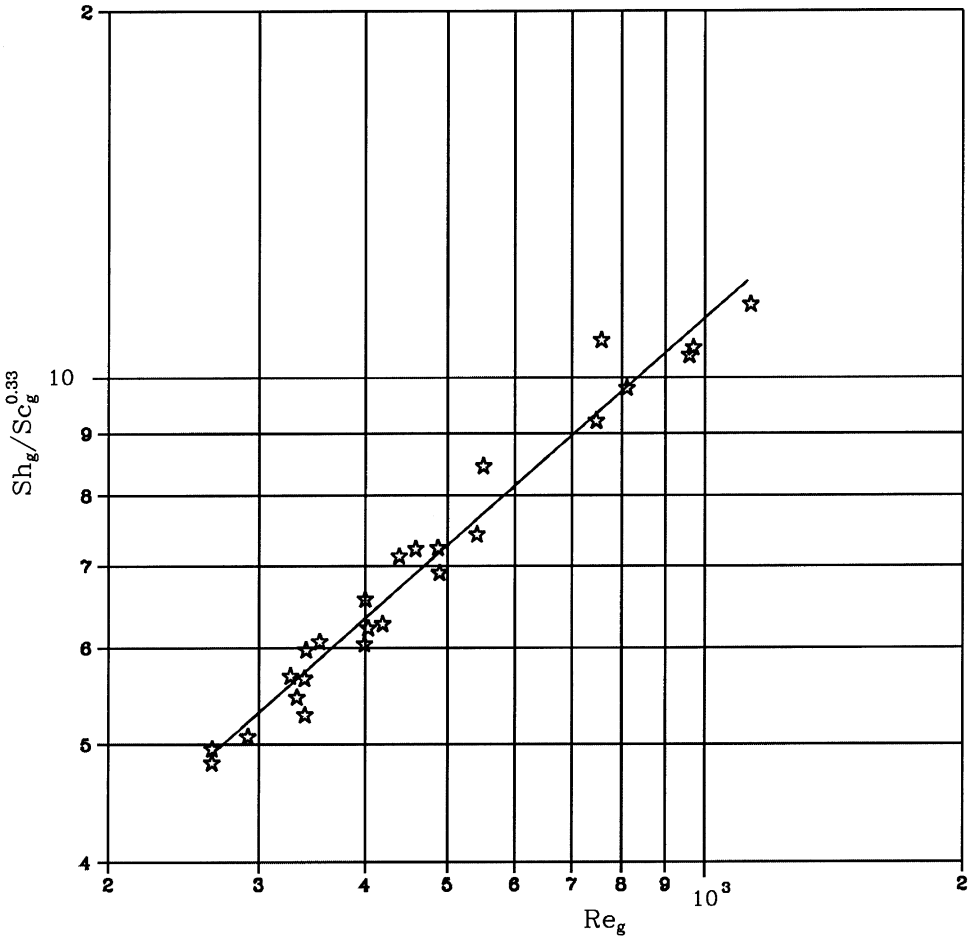

Fig. 8. Gas-phase mass transfer coefficients: Sherwood number vs. gas Reynolds number — upper range.

are usually less accurate than those for the mass transfer coefficients.

7. Mathematical model of catalytic distillation

A rigorous dynamic rate-based model for catalytic distillation processes as presented by Schneider et al. [5] was modified from the standpoint of the availability of model parameters for the catalytic packing. The model is based on the film theory and comprises the material and energy balances for an element of the two-phase volume in the packing as shown in Fig. 9. The interfacial flux is given by

$$N_i^j = \frac{\pi}{4} D_c^2 a \Delta z^j k^j (y_i^j - y_i^{j*}) + N_t^j \bar{y}_i^j \tag{16}$$

Material balances for the bulk phases, consider the chemical reaction in the liquid phase using the reaction kinetics presented by Pöpken et al. [6]:

$$G_g^j y_i^j = G_g^{j-1} y_i^{j-1} - N_i^j \tag{17}$$

$$G_L^j x_i^j = G_L^{j+1} x_i^{j+1} + N_i^j + \nu_i r m_{Kat}^j \tag{18}$$

The mathematical model presented above together with the experimental correlations for the mass transfer and pressure drop of MULTIPAK® have been incorporated into a simulation tool developed to reflect the strong physico-chemical interactions in

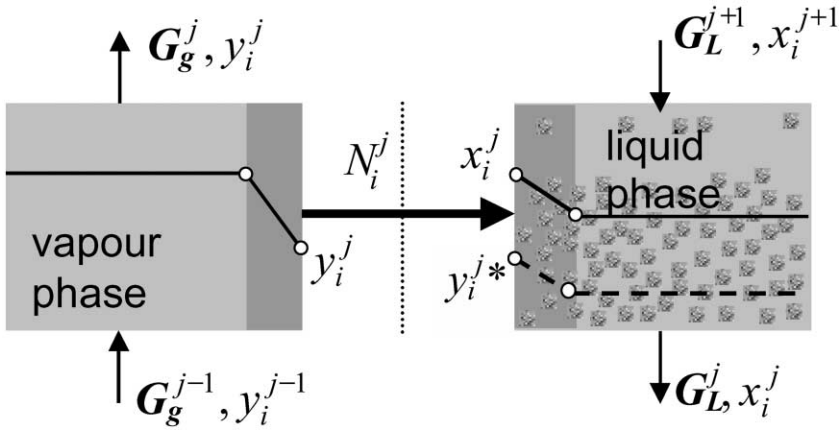

Fig. 9. Film model of the catalytic distillation process.

a catalytic distillation process. The simulation tool is able to calculate temperature and concentration profiles along the column as well as estimate the necessary reflux and boilup.

8. Experimental verification of the reactive distillation model

Simulation results for the production of methyl acetate have been compared with the experimental results obtained in a pilot-plant catalytic distillation column. The column has an inner diameter of 50 mm and a total packing height of 4 m which enables continuous operation. Process conditions are as follows: acetic acid feed of 1.3 kg/h, methanol feed of 0.7 kg/h, distillate flow of 1.65 kg/h and reflux ratio of 1.0. The appropriate remark has been done within the paper. A process-control system makes it possible to display and record all the relevant process data. Liquid-phase samples are taken along the column height and analysed via gas chromatography. For the synthesis of

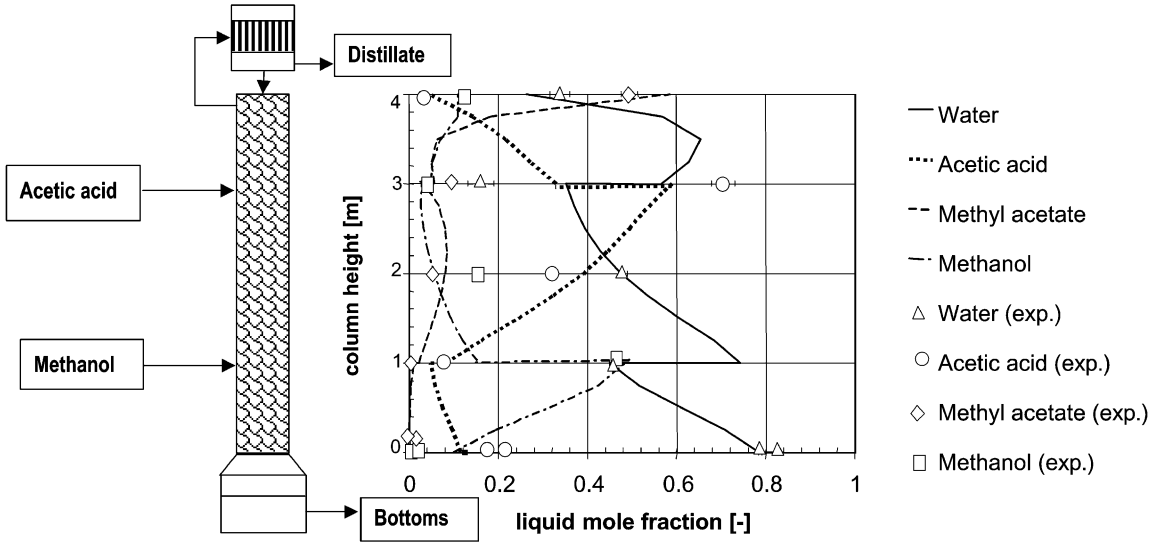

Fig. 10. Concentration profiles of the reactants along the column: calculated (lines) and experimental (points).

methyl acetate, a column configuration closely resembling that employed in industrial applications [5] has been chosen, with 2 m of the catalytic packing MULTIPAK® between the two feeds and 1 m above and below the reactive section. Acetic acid is fed to the column above the reactive section, while methanol is fed below. The test column is shown schematically on the left-hand side of Fig. 10.

A process simulation has been carried out with the simulation tool described above, leading to concentration profiles along the column (Fig. 10). Maximum concentrations of methanol and acetic acid can be observed at the respective inlets, while methyl acetate content increases towards the top and that of water increases towards the bottom of the column. The experimental data shown in Fig. 10 demonstrate that the theoretical results indeed reflect the actual process behaviour of methyl acetate synthesis, although deviations from the experimentally determined concentration profiles can still be observed, especially within the reactive section of the column. The investigated process of methyl acetate synthesis is strongly influenced by the reaction. A comparison of experimental and simulation results for the overall conversion are showing an experimental value of 82.7% in contrast to the simulation result of 90.8%. This phenomenon can be explained with a reduced activity of the catalyst inside the column but an extended data basis is needed to confirm this assumption.

9. Final remarks

The results of an extensive study concerning a new type of structured catalytic packing MULTIPAK® are presented in this paper. The main hydraulic characteristics of the packing, namely pressure drop for dry, prewetted and wetted packings as well as the flooding line have been determined experimentally. A very interesting effect has been observed — the pressure drop for the completely dry packing was higher than that for the prewetted packing and even higher than the pressure drop for low liquid loads in the two-phase flow — a phenomenon which has not been mentioned earlier in the literature. This could be caused by a thin layer of liquid present at the surface of wire gauze. The liquid film smoothes the coarse wire gauze surface; the large amount of liquid in the catalyst pockets forms the reservoir, protecting the film against drying. The plots of the friction factor for the dry and prewetted packings vs. Reynolds number resemble those for coarse and smooth tubes, respectively. It should be stressed that the MULTIPAK® has very small channels; for other catalytic packings (e.g. KATAPAK®-S) the phenomenon may not appear.

The mass transfer coefficients in the gas and liquid phases have been determined for the whole operating range of the packing. The correlations have been derived in terms of dimensionless numbers for the use during the modelling of the catalytic distillation process.

A simplified mathematical model has been formulated for the modelling of the catalytic distillation process. The model, together with the pressure drop and mass transfer correlations, has been incorporated into the simulation tool. Simulations have been performed for the synthesis of methyl acetate chosen as a test case.

The simulation tool has been verified using the experimental results for methyl acetate synthesis carried out in the laboratory-scale setup. The model reproduces the experimental data quite well, although deviations can still be observed, a phenomenon that might indicate a reduced activity of the catalyst material. It seems that further studies are necessary to develop a model that would better reflect the real process.

Acknowledgements

The paper presents a part of the project “Reactive packings” carried out within the framework of the Polish–German Scientific Network INCREASE.

References

[1] P. Moritz, H. Hasse, Chem. Eng. Sci. 54 (1999) 1367.
[2] I. Bylica, M. Jaroszyński, Inż. Chem. Proc. 3 (1995) 421–439.
[3] T. Hobler, Mass Transfer and Absorbers, WNT, Warszawa, 1966.
[4] M. Jaroszyński, I. Bylica, Inż. Chem. Proc. 18 (3) (1997) 427–438.
[5] R. Schneider, C. Noeres, L.U. Kreul, A. Górak, Comput. Chem. Eng. 23 (Suppl.) (1999) 423.
[6] T. Pöpken, L. Götze, J. Gmehling, Ind. Eng. Chem. Res. 39 (2000) 2601.